Zero-Order Interfacial Enzymatic Degradation of Phospholipid Tubules

Paul A. Carlson,* Michael H. Gelb,‡ and Paul Yager*
*Molecular Bioengineering Program, Department of Bioengineering, and ‡Departments of Chemistry and Biochemistry, University of Washington, Seattle, Washington 98195 USA

ABSTRACT The first study of enzymatic hydrolysis of phospholipid tubules is reported. Phosphatidylcholines with acyl chains containing diacetylene groups are known to form tubular microstructures in which the lipids are tightly packed and crystalline. These tubules can be used to probe the role of microstructural form in the mechanics of interfacial enzymatic degradation by such enzymes as phospholipase A_2 (PLA_2). Hydrolysis by PLA_2 may occur most rapidly in regions having the greatest number of bilayer packing defects, such as those that must be found at tubule ends. A microstructure that degrades primarily from its ends should exhibit zero-order kinetics, because the area of the degrading tubule end remains constant as the length of the microstructure decreases. Free fatty acid concentration was measured to follow the generation of PLA_2 hydrolysis products in suspensions of diacetylenic phospholipid tubules. The kinetics of tubule hydrolysis were essentially zero-order until conversion was complete, as predicted. However, microscopy of partially hydrolyzed tubules revealed the formation of multiple discrete anionic product domains along the length of degrading tubules as well as in insoluble reaction product microstructures. Furthermore, the rate of tubule hydrolysis was only moderately enhanced by increasing the number of tubule ends, which is consistent with the conclusion that tubule ends are not the only sites of hydrolysis. A model that reconciles the overall kinetics with the morphological evidence is proposed.

INTRODUCTION

Phospholipase A_2 (PLA_2), a phospholipid hydrolase, is the best-characterized interfacial enzyme (Gelb et al., 1995; Jain et al., 1995). However, the mechanistic details of how molecular packing irregularities within a homogeneous bilayer phase (e.g., those occurring at phase boundaries and structural defects) facilitate hydrolysis are still controversial. Studies using phosphatidylcholine (PC) monolayers dispersed at the air-water interface compressed within the gel-liquid crystalline phase coexistence region demonstrate that hydrolysis occurs at specific sites on phase boundaries (Grainger et al., 1990; Maloney et al., 1995; Reichert et al., 1992). For bilayer systems, dispersions of small unilamellar PC vesicles below the phospholipid melting temperature (T_m) show accelerated rates of hydrolysis compared to multilamellar systems, putatively because of their greater density of packing defects caused by high bilayer curvatures (Burack and Biltonen, 1994; Burack et al., 1993; Wilschut et al., 1978). Collectively, these data hint that phase boundaries and packing irregularities are important facilitators of enzymatic hydrolysis at interfaces.

Phosphatidylcholines with acyl chains containing diacetylene groups are known to form tubular microstructures consisting of tightly packed, crystalline lipids (Caffrey et al., 1991; Schnur, 1993; Schnur et al., 1987; Thomas et al., 1995; Yager and Schoen, 1984). Tubules provide an attractive microstructure for exploring the role of packing defects on hydrolysis kinetics because, unlike a dispersion of vesicles, all of the substrate in a single-walled tubule is immediately accessible to enzyme, and all phospholipid molecules experience the same bilayer curvature. Even in multiwalled tubules, permeation of enzyme from the edges of tubules should provide eventual access to all substrate. Furthermore, lipid tubules make excellent model systems for studying the role of packing heterogeneity in interfacial catalysis by PLA_2; hydrolysis should be favored in bilayer regions with a high density of packing defects, such as those found at the tubule ends. If hydrolysis occurs most predominately from the tubule ends inward, then the kinetics could be zero-order, because the number of substrate molecules accessible to enzyme at the tubule ends remains constant as the length of the substrate microstructure decreases, as in Fig. 1.

Lipid tubules were first characterized over a decade ago in dispersions of the phospholipid 1,2-bis(10,12-tricosadiynoyl)-*sn*-glycero-3-phosphocholine ($DC_{8,9}PC$) (Schnur, 1993; Thomas et al., 1995; Yager and Schoen, 1984). Formation of these microstructures was achieved either by conversion to a tubule microstructure via a lipid phase transition during cooling of a high-temperature aqueous dispersion of liposomes (Yager and Schoen, 1984), or by water-induced precipitation of tubules directly from a water-miscible solvent such as ethanol (Georger et al., 1987; Thomas et al., 1995). The tubule morphology is composed of helically wrapped lipid bilayers that close to form straight, hollow, rigid tubes. $DC_{8,9}PC$ tubules are ~0.75 μm in diameter, vary in length from a few microns to nearly 1 mm, and are either uni- or multilamellar, depending on the formation conditions. X-ray diffraction data suggest a high degree of conformational order of the lipids packed within tubules, whereas infrared and Raman spectroscopic studies indicate that the acyl chains of $DC_{8,9}PC$

Received for publication 7 October 1996 and in final form 16 April 1997.
Address reprint requests to Dr. Paul Yager, Center for Bioengineering, University of Washington, Box 352255, Seattle, WA 98195. Tel.: 206-543-9374; Fax: 206-543-6124; E-mail: yager@bioeng.washington.edu.

0006-3495/97/07/230/09 $2.00

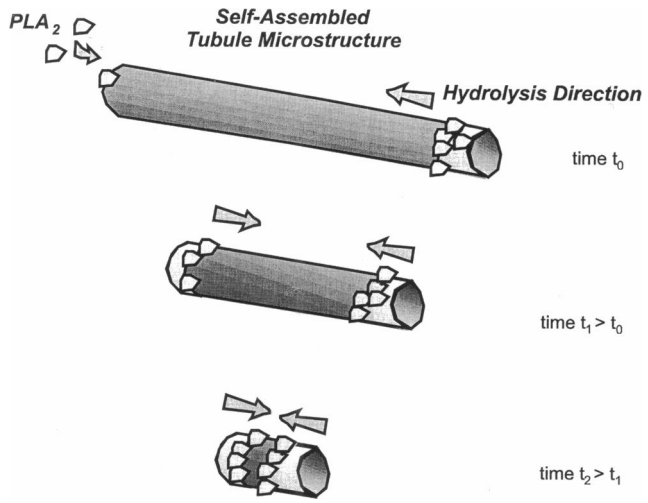

FIGURE 1 Cartoon showing a hypothetical mechanism for lipid tubule hydrolysis catalyzed by PLA_2, which would give rise to zero-order kinetics. The kinetics could be zero-order if the number of substrate molecules accessible to enzyme at the tubule ends were to remain constant as the length of the substrate microstructure decreases. Bilayer packing heterogeneity should be greatest at the tubule ends, and the rate of interfacial catalysis by PLA_2 in these disordered regions should dominate the hydrolysis kinetics.

microstructures exhibit tight chain packing (Schnur et al., 1987; Caffrey et al., 1991). Even though the membrane has been characterized as a highly ordered lamellar-crystalline bilayer, tubules often appear in the presence of minority structures such as open helical ribbons (Georger et al., 1987). Helical striation patterns on the outside of closed tubules (i.e., molecular packing defects) are often observable by electron microscopy, as they are in tubule samples used in this work. The tubule structure is, therefore, somewhat polymorphic, and although there have been several theoretical models proposed for tubule structure and formation (Chappell and Yager, 1991; Selinger and Schnur, 1993), there remain several questions about the structure of $DC_{8,9}PC$ tubules and helices. The suggestion by Selinger et al. that continuous, defect-free $DC_{8,9}PC$ tubules with no striation patterns have a molecular packing order different from that of tubules that are clearly made up of helically wrapped bilayers is controversial, but not inconsistent with observed data (Selinger and Schnur, 1993). Despite these subtle uncertainties in their molecular structure, lipid tubules represent a unique microstructure for studying the role of bilayer packing defects and phase boundaries in interfacial hydrolysis kinetics.

Initially we made the simplifying assumption that all tubules are strictly cylindrical, with smooth defect-free walls that consist of monodomain crystals. The tight crystalline packing of the tubule wall would prevent both dissolution of monomeric lipid and enzymatic hydrolysis of the lipids, except at the edges at the tubule ends. To control for the fact that tubules exist as crystalline lipids only below T_m, we also studied a gel-phase phospholipid system with a radically different microstructure: small unilamellar vesicles (SUVs) prepared from 1,2-dipalmitoyl-*sn*-glycero-3-phosphocholine (DPPC). The T_m of DPPC at 41.3° (Small, 1986) is similar to that of $DC_{8,9}PC$ and is only slightly depressed in SUVs. Because they have identical headgroups and because PLA_2 is known to be relatively insensitive to the nature of the phospholipid hydrocarbon chain, comparison of hydrolysis of DPPC vesicles and $DC_{8,9}PC$ tubules allows isolation of those effects unique to a tubular microstructure during hydrolysis from those due to different headgroup chemistries.

MATERIALS AND METHODS

$DC_{8,9}PC$ was obtained from Avanti Polar Lipids (Birmingham, AL) as a dry powder. Thin-layer chromatography (TLC) using chloroform:methanol:water (65:35:5) showed no hydrolysis product spots, and the lipid was used without subsequent purification. Suspensions of $DC_{8,9}PC$ tubules were prepared by precipitation of the solvated lipid from ethanol with dropwise addition of water (Georger et al., 1987). Deionized water was added to a 5 mM solution of the lipid in ethanol until the volume fraction of water in ethanol reached 70%; precipitation occurred, and the solution became turbid. The microstructures were allowed to anneal in the 70% ethanol solution for 1 week at room temperature. Ethanol was removed by a series of centrifugation and resuspension steps in distilled water. For the final exchange, the pellet of tubules was resuspended in isotonic digestion buffer (10.0 mM Tris-HCl, 10 mM $CaCl_2$, 150 mM NaCl, and 0.01 weight% sodium azide, pH 8.5). To create a suspension of $DC_{8,9}PC$ tubules with a smaller distribution of tubule lengths, a portion of the buffered stock $DC_{8,9}PC$ suspension was sonicated in an ice bath for 5 min. DPPC (obtained from Avanti Polar Lipids) was dissolved in chloroform. TLC showed no hydrolysis product spots, and this lipid was used without purification. DPPC was dried from chloroform to create a 5 mM stock solution upon resuspension with the isotonic digestion buffer. To create a suspension of SUVs, the buffered DPPC suspension was sonicated for 30 min at 50° until it clarified.

Measurement of phospholipid hydrolysis kinetics

Hydrolysis studies on $DC_{8,9}PC$ tubule and DPPC SUV suspensions by PLA_2 were performed as follows. For all PLA_2 reactions, 0.5 mM $DC_{8,9}PC$ and DPPC dispersions were diluted from stock lipid suspensions with the isotonic digestion buffer. Reaction mixtures of 25 ml were placed in amber reaction flasks to reduce photopolymerization of the reaction products, and each mixture was preheated to 30°C before the addition of PLA_2. At time 0, *Naja naja kaouthia* (cobra venom) PLA_2 (Sigma Chemical Co., St. Louis, MO) was added to a concentration of 2.24 μg/ml (160 nM) to start hydrolysis. For fatty acid determination, a 25-μl aliquot was removed and added to a 25-μl solution containing 20 mM EDTA, which was needed to chelate Ca^{2+} and to stop further hydrolysis, and 5 mM Triton X-100 (TX100) detergent. The mixture was heated above the phospholipid T_m (e.g., greater than 45°C for both $DC_{8,9}PC$ and DPPC) in a 10-fold molar excess of Triton X-100 (TX100) detergent to solubilize the microstructures formed during hydrolysis and to release any fatty acid trapped within the microstructures. This micellar dispersion was added to a fluorescence cuvette containing 1.5 ml of the 0.2 μM ADIFAB buffer (Molecular Probes, Eugene, OR) to determine the concentration of fatty acid reaction products.

The ADIFAB assay is based on a fatty acid-binding protein, which has been covalently modified with the fluorescent dye Acrylodan. The binding of a fatty acid to the modified protein induces a shift in fluorescence emission from 432 nm to 505 nm; the ratio of these emission intensities provides a measure of the concentration of fatty acid bound to the protein. The total fatty acid concentration during lipid hydrolysis was determined by the ADIFAB binding assay with a Perkin-Elmer LS-5B luminescence

spectrometer. A titration curve created from the spectral response of ADIFAB in the presence of both EDTA and TX100 detergent to known concentrations of fatty acid was used to determine the total amount of fatty acid formed during hydrolysis. The ratiometric fluorescence response of ADIFAB to increasing concentrations of 10,12-tricosadiynoic acid is linear up to a concentration of 40 μM, where the response reaches a plateau, which results when fatty acid micelles form. The response of ADIFAB to palmitic acid is similar. As such, samples taken during hydrolysis were diluted up to a factor of 16 to measure fatty acid concentrations greater than 40 μM. Concentrations of 10,12-tricosadiynoic acid and palmitic acid were determined throughout hydrolysis from the ratio of fluorescence intensities measured at 505 nm and 432 nm and the calibration curve.

Microscopic examination of hydrolysis microstructures

During the course of $DC_{8,9}PC$ hydrolysis, 25-μl aliquots of the digest solution were removed for examination by transmission electron microscopy. Samples for transmission electron microscopy (TEM) were prepared by applying the aliquots to Formvar-coated 150-mesh copper TEM sample grids and staining with an aqueous 1.5% ammonium molybdate solution. The samples were stored in a sample grid box before observation with a Philips EM 410 electron microscope. Samples for fluorescence microscopy were prepared by mixing a 25-μl aliquot sample taken from the digest solution with 25 μl of a hydrolysis quenching buffer that contained 10 mM Tris-HCl (pH 8.5), 150 mM NaCl, 20 mM EDTA, and 0.01% NaN_3. The quenched samples were stained with the cationic fluorescent dye H379 (Molecular Probes). Contrast was enhanced in regions of the microstructures where anionic fatty acids had accumulated by mixing 50 μl of 10 mM Tris-HCl (pH 8.5) buffer containing 100 ng/ml of H379 with the PLA_2-quenched digest sample. Images were taken with a DAGE 66 SIT camera attached to a Zeiss epifluorescence microscope and were digitized by a frame grabber on a Macintosh II microcomputer.

Calorimetry

Differential scanning calorimetry (DSC) studies were performed with a Seiko Instruments (Torrance, CA) DSC100 differential scanning calorimeter connected to a Seiko Instruments SSC-5020 thermal analysis system. Samples were prepared by transferring 70-μl aliquots of the original tubule suspension and the suspension of PLA_2 hydrolysis products into silver DSC pans. Each pan was immediately sealed and transferred to the calorimeter, which was warmed to 25°C. A 70-μl aliquot of the isotonic digest buffer was used as the reference. Samples were scanned at a rate of 0.5°/min for both heating and cooling cycles. The heating transition temperatures were determined from the onset of the transition endotherms.

Fluorescent labeling of PLA_2

The succinimidyl ester of carboxyfluorescein (Molecular Probes) was coupled to PLA_2. Approximately 560 μg of *Naja naja kaouthia* cobra PLA_2 (Sigma Chemical Co.) were dissolved in 1 ml of 100 mM sodium borate buffer (pH 9.3). The dye (succinimidyl ester) was dissolved in 1 ml of dimethyl sulfoxide to a final concentration of 21.1 mM, and a 2.1-μl aliquot of this solution was added to the buffered protein solution (dye/protein ratio of 1.5:1). The reaction mixture was incubated at room temperature for 3 h and then, to separate unincorporated dye, was run over a Sephadex G-25M column (Pharmacia Biotech, Uppsala, Sweden) that had been equilibrated with distilled water. The protein was lyophilized and then resuspended in aqueous buffer consisting of 10 mM Tris-HCl (pH 8.5) in the presence of 10 mM $CaCl_2$, 150 mM NaCl, and 0.01% sodium azide. The unconjugated enzyme and fluorescein-conjugated enzyme showed similar activities toward DPPC, as determined by the Sigma Chemical Co. protocol for PLA_2 activity.

RESULTS

The microstructural form into which phospholipids self-assemble strongly influences the kinetics of hydrolysis. Fig. 2 shows the progress curves for the hydrolysis of 0.5 mM dispersions of DPPC SUVs and of multilamellar $DC_{8,9}PC$ tubules at 30°C by 2.24 μg/ml PLA_2, as determined by the production of free fatty acid (Richieri et al., 1992, 1993). The hydrolysis progress curve for the control SUV dispersion of DPPC was biphasic. Biphasic behavior is consistent with the types of hydrolysis profiles reported by Biltonen's group and others (Burack and Biltonen, 1994; Burack et al., 1993; Wilschut et al., 1978). An initial rapid hydrolysis stage, which ends after roughly 50% of the total lipid has been hydrolyzed, is followed by a period of slower, nearly constant hydrolysis. In a unilamellar liposome, only the outermost monolayer is initially accessible to enzyme. The rapid initial hydrolysis rate of 0.88 s^{-1} reflects the hydrolysis of lipids in the outer monolayer. The onset of the subsequent slower hydrolysis stage is caused by substrate depletion in the outer monolayer. Hydrolysis proceeds to completion at ~0.044 s^{-1}, limited by access to new substrate either from the bursting of partially hydrolyzed vesicles or from slow phospholipid flip-flop between the inner and outer vesicle monolayers.

The progress of $DC_{8,9}PC$ tubule hydrolysis is markedly different from that of DPPC liposomes. A lag before the rapid hydrolysis phase is common to many PLA_2-catalyzed PC reaction profiles (Burack et al., 1993; Gelb et al., 1995; Jain et al., 1995), although the duration of the lag phase in liposomes is much shorter. After a 2.5-h lag, the hydrolysis proceeds with a slow, nearly constant rate of 0.13 s^{-1} for most of the reaction. The rate of hydrolysis of $DC_{8,9}PC$

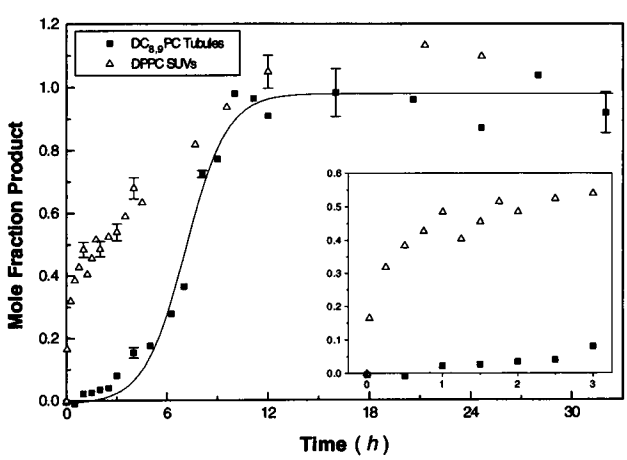

FIGURE 2 The total hydrolysis progress curves for $DC_{8,9}PC$ tubule suspensions and DPPC SUV suspensions by PLA_2. Each point within the progress curves was determined by the acrylodated-intestinal fatty acid binding protein (ADIFAB) assay for free fatty acid hydrolysis products. (*Inset*) The rapid initial DPPC hydrolysis phase and the initial $DC_{8,9}PC$ lag phase. The reaction progress curve for DPPC was biphasic, and the reaction progress curve for $DC_{8,9}PC$ tubules was linear, which was consistent with our model for tubule hydrolysis.

tubules after the initial lag is 6.8 times slower than that for the outermost DPPC vesicle monolayer, and in contrast to all other reported PLA_2 reaction profiles, it remains constant after the initial lag until nearly 100% hydrolysis. This constant hydrolysis rate is consistent with our simple mechanistic model of end-dominated tubule hydrolysis.

Our model predicted that a tubule would degrade by shortening with time as reaction products leave from the eroding ends. However, equimolar mixtures of fatty acids and lysophosphatidylcholines are known to form a bilayer, even though the individual components form micelles when dispersed in water (Jain et al., 1980). Mixtures of fatty acids and lysophosphatidylcholines exhibit twin endothermic transitions at temperatures higher than that of the corresponding phosphatidylcholine (Mabrey and Sturtevant, 1977). DSC studies of the $DC_{8,9}PC$ tubules and the end-stage hydrolysis products confirmed that the products do not dissolve, but remain within the microstructure. DSC heating traces of the end-stage hydrolysis products of $DC_{8,9}PC$ tubules feature a large, broad endotherm at an onset temperature of 69.8°C, which is much higher than the T_m of 43.8°C measured for unhydrolyzed $DC_{8,9}PC$ tubules. This is consistent with the existence of end-product bilayers.

The microstructures observed in TEM of partial digests, as in Fig. 3, reflect that shortly after the addition of enzyme, helical ribbons emerge from what appear to be fractured tubules. Even though a few intact tubules are still present at the 50% hydrolysis point, the types of microstructures present include small filaments, helical ribbons, and elongated sheets. Near completion, the reaction mixture contains a rich variety of microstructures. Tubules do not simply shorten by dissolution of hydrolysis reaction products from their ends.

Because tubule hydrolysis was studied in pH 8.5 buffer, the diacetylenic fatty acid reaction products should be at least partially charged in the bilayer. The cationic fluorescent dye, 1,1,3,3,3′,3′-hexamethyl-indocarbocyanine iodide (H379) was added to visualize regions of negative charge

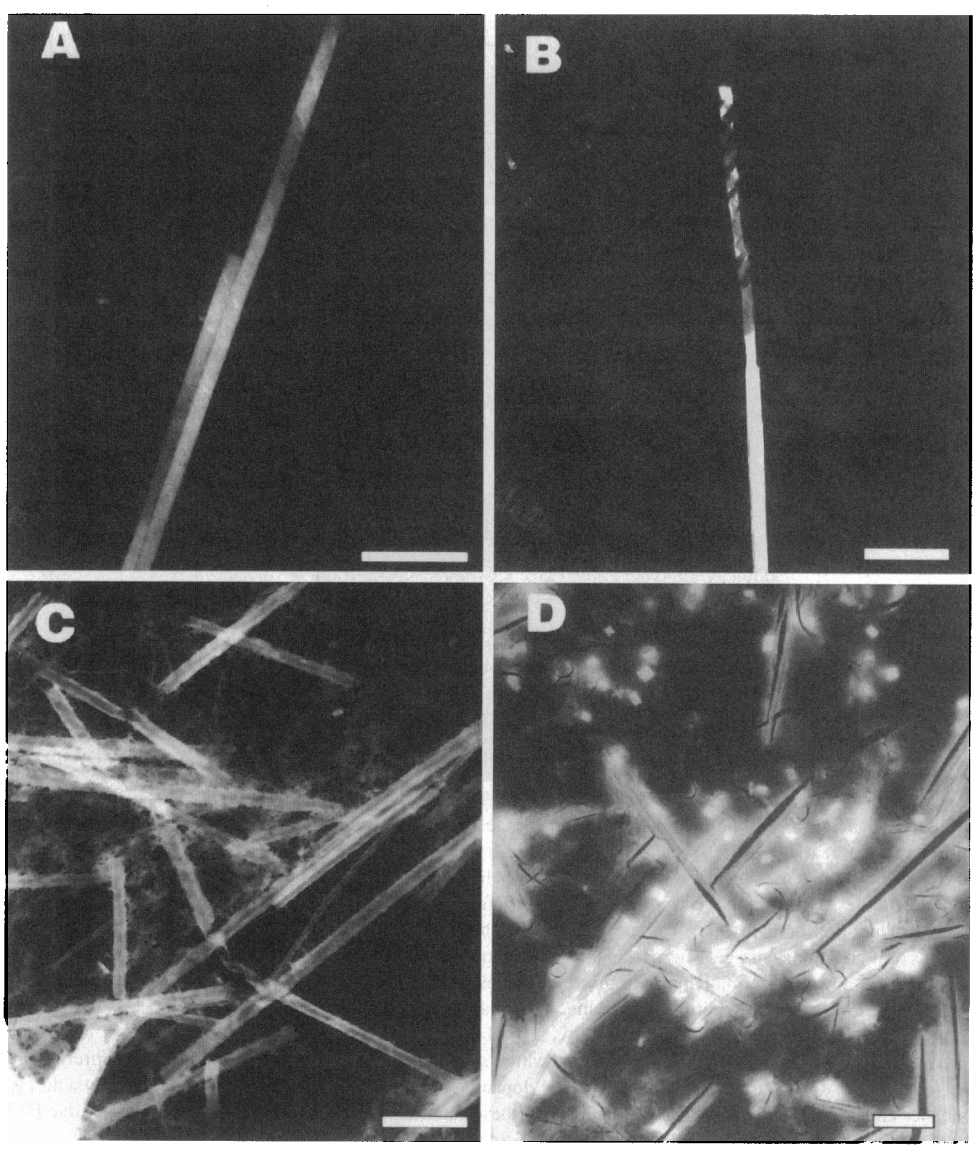

FIGURE 3 A time series of negative-stain transmission electron micrographs during the hydrolysis of $DC_{8,9}PC$ lipid microstructures taken (*A*) 0 h, (*B*) 1 h, (*C*) 3 h, and (*D*) 8 h after the addition of enzyme. An aqueous solution of 1.5% ammonium molybdate was used as a negative stain. The micrographs taken of samples at time periods greater than 8 h (not shown) contained a larger fraction of ribbon, sheet, and filament microstructures, but were very similar in appearance to micrograph *D*. Notice that the tubule microstructure in *A* contains evidence of helical defects on the tubule face (e.g., striation patterns), even before the addition of enzyme. Evidence of tubule fracture appears early in the course of hydrolysis (*B*), and this process continues with time. Scale bar: 5 μm

accumulation (Grainger et al., 1990). Immediately after the addition of enzyme, the fluorescence images show a homogeneously dark field of view with no tubules visible, and the cationic dye shows no association with the tubules. The series of fluorescence and phase-contrast optical micrographs in Fig. 4 show product domain formation within the microstructures. Early in the reaction, discrete fluorescent regions appear at several points along intact tubules. Although hydrolysis does progress along the tubule surface, its initiation is not limited to tubule ends. If local defects in molecular packing within the bilayer function as initiation sites for hydrolysis, there must be packing defects at multiple sites along many of the tubules in this type of preparation. Alternatively, the sample is dominated by multila-

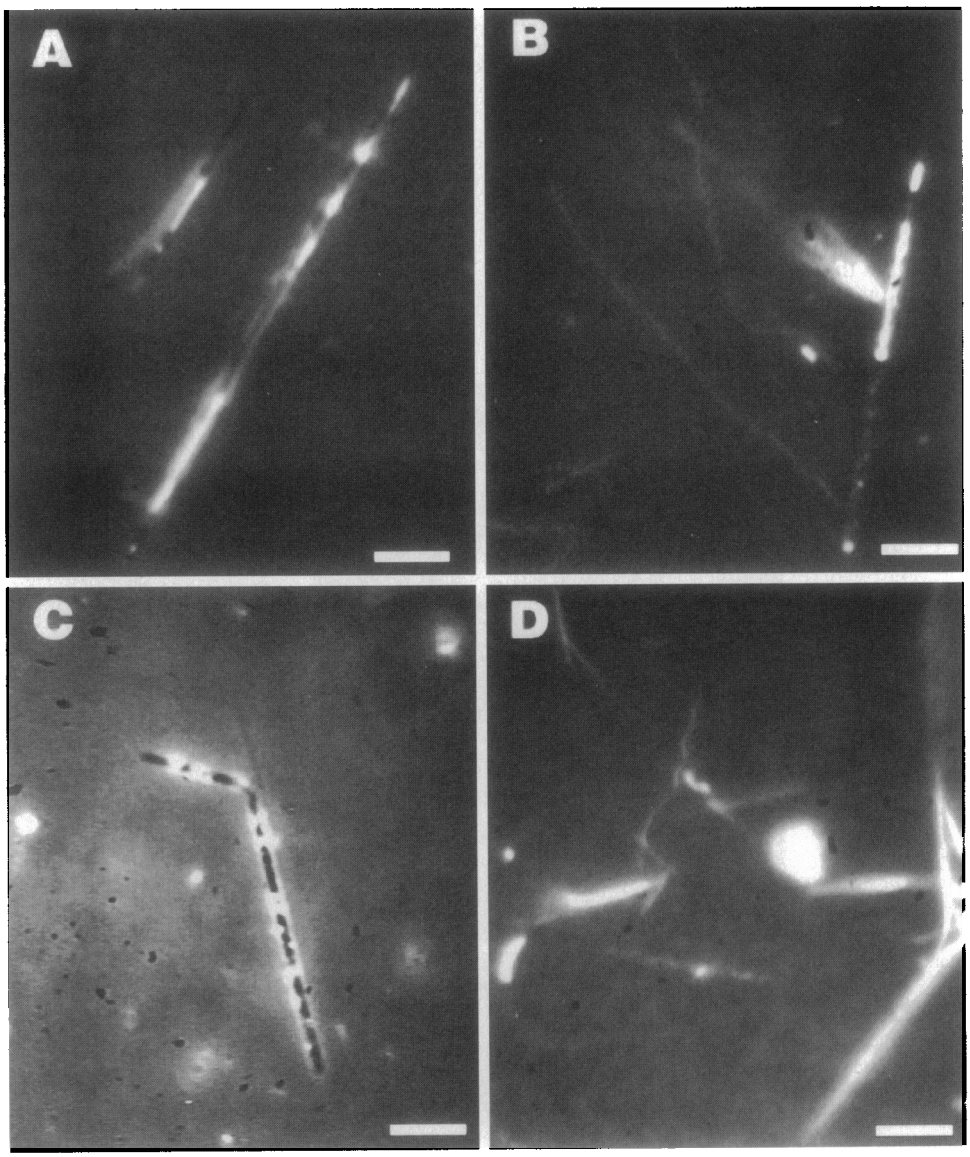

FIGURE 4 Digitized phase-contrast and fluorescence micrographs showing product domains within the $DC_{8,9}PC$ microstructures, as indicated by the cationic fluorescent dye H-379, which enhances contrast in regions where anionic fatty acids have accumulated. At time 0 h, immediately after the addition of enzyme, the fluorescence images (not shown) show a homogeneously dark field of view with no tubules visible, and the cationic dye shows no association with the tubules. Micrograph *A* is a combined phase-contrast and fluorescence image of the original tubule suspension taken 1 h after the addition of enzyme, when product-rich domains have started to form. The bright spots are from the fluorescence emission of the cationic dye H379, which associates with regions of high anionic charge. Micrograph *B* is a combined phase-contrast and fluorescence image of the tubule suspension 3 h after the addition of enzyme. Most tubules now appear splotchy, with discrete regions of reaction product accumulation. Micrograph *C* is a combined phase-contrast and fluorescence image taken 5 h after the addition of enzyme. The image contains a microstructure that appears to have unwrapped and twisted upon exposure to the fluorescence excitation source. Micrograph *D* is a combined phase-contrast and fluorescence image taken 10 h after the addition of enzyme. Most of the microstructures visible are strongly fluorescent, which suggests that they are product-rich if not entirely composed of reaction products. Tubules can be prepared with a small mole fraction of fatty acid dopant ($\chi_{FA} < 0.1$). Higher mole fractions of fatty acid ($\chi_{FA} > 0.1$) solubilize tubules to form mixed micelles and other nontubule microstructures. Under these conditions and in the presence of the cationic dye H379, the tubules appear uniformly fluorescent, with no discernible product domains (not shown). Scale bar: 5 μm

mellar tubules, which can have multiple bilayer ends along their length. The highly fluorescent helical ribbon, flat sheet, and other small fibrous microstructures seen at later times, like those seen with TEM, must contain a high level of reaction products. Interestingly, tubules can be formed along with a small mole fraction of 10,12-tricosadiynoic acid dopant ($\chi_{FA} < 0.1$) without disruption of the tubule microstructure. Tubules, in the presence of the fatty acid dopant and H379, appear uniformly fluorescent with no discrete product domains (images not shown).

Grainger et al. observed that as hydrolysis by PLA_2 of phosphatidylcholine monolayers at the air-water interface progresses, the enzyme becomes increasingly localized within product-rich domains (Grainger et al., 1990; Maloney et al., 1995). Distortions in membrane structure from localized packing defects, phase separation of reaction products, and changes in membrane curvature may lead to recruitment of additional PLA_2 to the membrane surface. Enhanced binding of PLA_2 to product-rich domains may also affect the hydrolysis profile observed for $DC_{8,9}PC$ tubules. An increase in concentration of enzyme within a localized zone of hydrolysis could accelerate the rate as long as there is adequate access to fresh substrate. To track the distribution of enzyme, 5-carboxyfluorescein-tagged PLA_2 was used. Fig. 5 shows that immediately after addition, PLA_2 distributes uniformly but weakly over the tubule surface. By the completion of hydrolysis, the product microstructures (i.e., helical ribbons and filaments) show strong fluorescence, which implies enhanced PLA_2 binding to product-rich microstructures. It is unclear, however, whether the accumulation of protein seen within product-rich domains results from recruitment of fresh, active enzyme to the membrane surface. In addition, there is a possible artifact in the fluorescent micrographs, because domains rich in diacetylenic fatty acid hydrolysis product can photopolymerize under bright blue microscope illumination. This polymer is also fluorescent. However, the rate of polymerization is very slow (i.e., on the order of a few minutes) compared to the rate at which fluorescein-labeled enzyme photobleaches.

If the molecular disorder, which is intrinsic to a crystalline domain boundary like those found at the tubule ends, drives PLA_2 hydrolysis of gel-phase phospholipids, then increasing the number of ends at a constant phospholipid concentration should increase the hydrolysis rate. Sonication of tubule dispersions at low temperatures fractures the tubules and greatly increases the number of tubule ends, as shown in Fig. 6. The hydrolysis rate for 4-μm-long tubules was twice that for 40-μm-long tubules. Clearly, there is an edge dependence to the hydrolysis rate, but not to the extent predicted by the change in the number of tubule ends alone. Sonication may have fractured the tubules in regions already containing a high concentration of molecular packing defects, which would have otherwise served as sites for hydrolysis initiation.

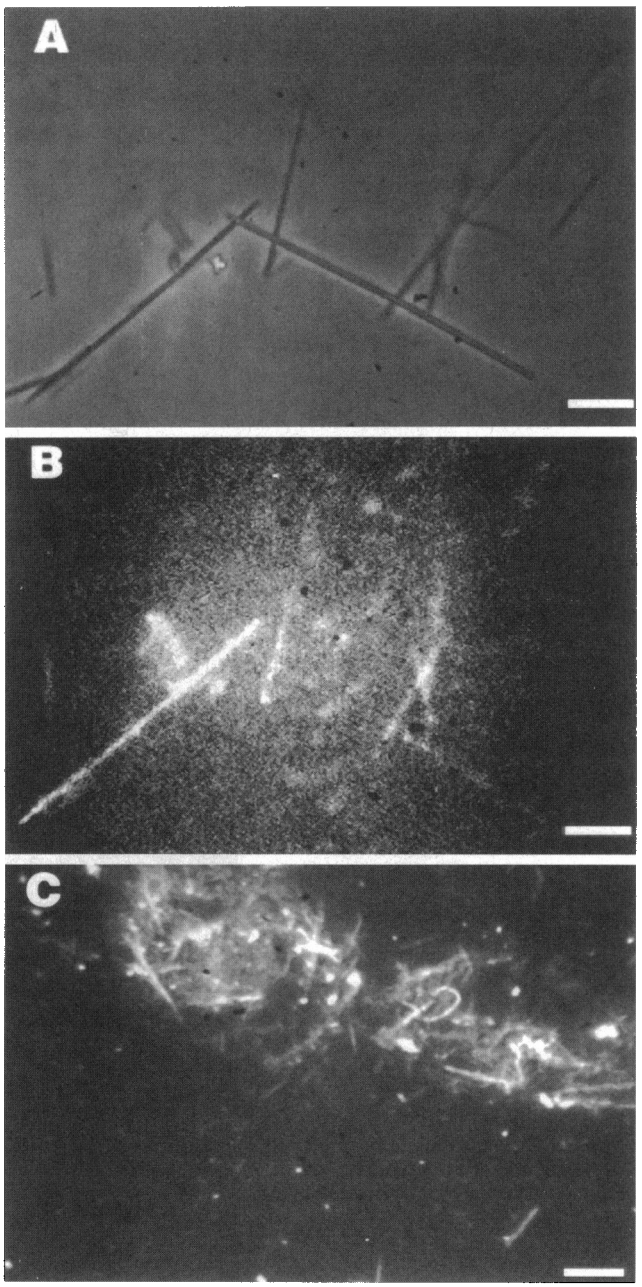

FIGURE 5 Digitized and image-enhanced phase-contrast (*A*) and fluorescence (*B* and *C*) optical micrographs taken of $DC_{8,9}PC$ tubules in the presence of 5-carboxyfluorescein-labeled PLA_2. Micrograph *A* is a phase-contrast image of the $DC_{8,9}PC$ tubule suspension after the addition of enzyme. Micrograph *B* is the corresponding digitally enhanced fluorescence image taken of the tubule suspension presented in *A*. Initially the enzyme binds uniformly to the lipid tubule substrate, but the fluorescence is very weak, which suggests a weak association between enzyme and tubules. Micrograph *C* is a fluorescence image of hydrolyzed tubules taken 20 h after the addition of enzyme. At the end of hydrolysis, the enzyme can be seen to be strongly associated with microstructures that are characteristic of those containing large amounts of reaction products. Scale bar: 5 μm

DISCUSSION

It is remarkable that an oversimplified model correctly predicts the constant hydrolysis rate of a polydisperse sam-

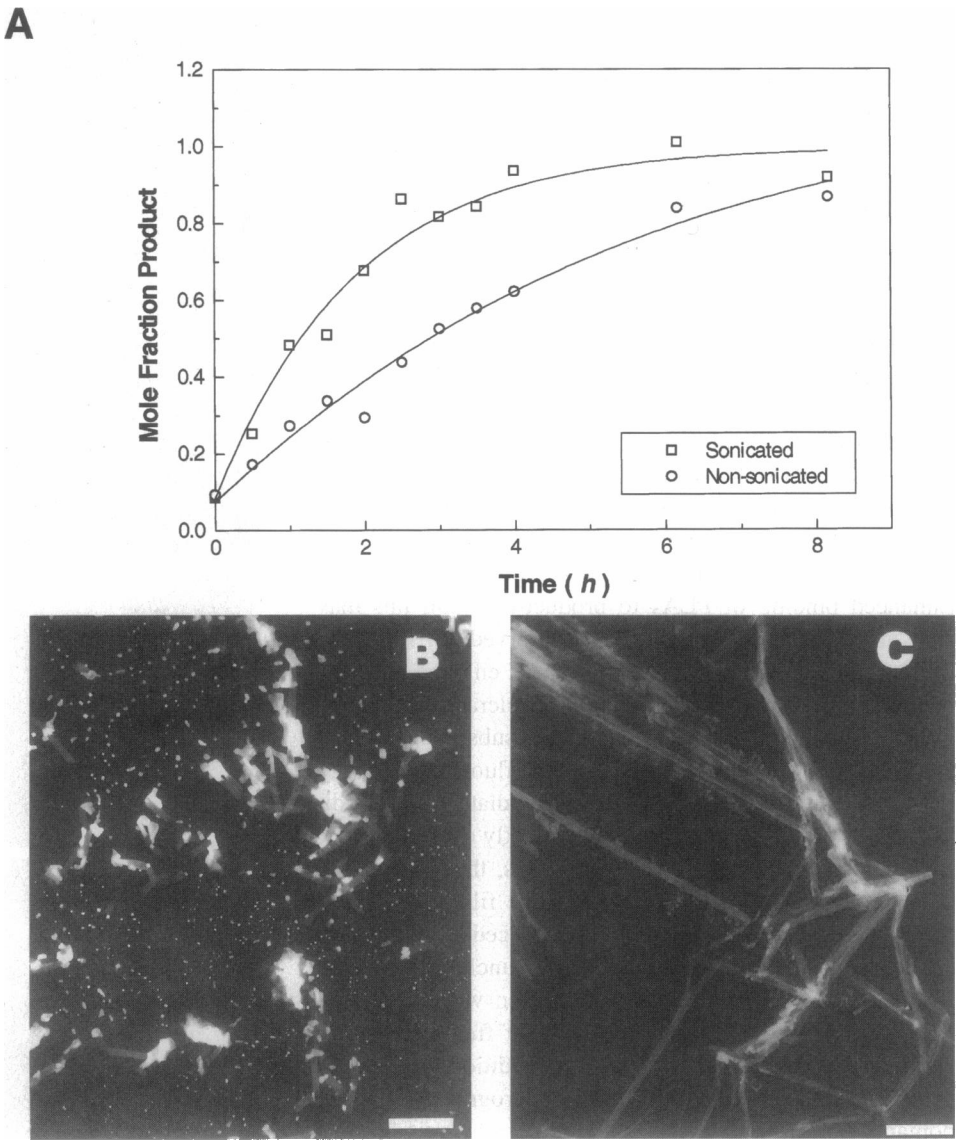

FIGURE 6 The hydrolysis profiles (*A*) for two suspensions of $DC_{8,9}PC$ lipid tubules with different mean tubule lengths: 4 μm (*B*) and 40 μm (*C*) as determined by TEM. The reaction buffer (pH 8.5) contained 10 mM Tris-HCl (pH 8.5), 150 mM NaCl, 5 mM $CaCl_2$, 0.01% sodium azide, and 0.5 mM lipid. The concentration of PLA_2 in the digest buffer was 2.24 μg/ml (160 nM). Each point within the progress curves was determined by the ADIFAB assay for free fatty acid hydrolysis products. The population with the 10× shorter mean tubule length has only a 2× faster rate of hydrolysis, which suggests that the number of tubule ends plays only a modest role in hydrolysis. Each tubule preparation had an initial mole fraction fatty acid greater than 0.05, and the subsequent hydrolysis profiles of the preparations lacked the distinctive lag phase. Scale bar: 5 μm

ple of $DC_{8,9}PC$ tubules, even though hydrolysis does not occur exclusively from the ends. A revised qualitative model of tubule biodegradation may be more correct. The assumption that packing defects in tubules occur predominantly at their ends is certainly inaccurate for the preparation of tubules used in this study because, as mentioned, they manifested distinct helical markings. An alternative model in which all tubules can have helical line defects corresponding to the edges of the helices occasionally seen in the tubule walls is attractive, but was not well supported by the optical microscopic images of partially hydrolyzed tubules. A more realistic approach is to model this tubule preparation as a mixture between smooth tubules (with their only defects at their ends) and partially annealed helices (with continuous defects along their lengths). Tubule hydrolysis by PLA_2 exhibits zero-order kinetics because the reaction proceeds by a processive mechanism from a few discrete sites on the tubule surface after the enzyme binds and hydrolysis begins.

The formation of product domains within tubules, as observed using epifluorescence microscopy and a cationic fluorescent dye, gives some insight into the mechanism of PLA_2 acting on tubule substrates. Product domains, which form early, must originate either from the processive action of PLA_2 (i.e., continuous hydrolysis without desorption of enzyme into the aqueous phase) along the surface, or from lateral phase separation of reaction products within the bilayer after hydrolysis. Given that the T_m of the reaction products is very high and that tubule $DC_{8,9}PC$ lipids are known to be rigid (Plant et al., 1990), lateral movement of the lipids within the tubule bilayer required to form a product domain is very unlikely. Domains form because enzymes "scoot" along the surface, processively converting the bilayer surface from $DC_{8,9}PC$ substrate to regions rich in reaction products.

The mechanisms giving rise to the rich variety of microstructures that arise as tubule hydrolysis progresses are not fully understood. The morphological changes of fluid lipid

vesicles throughout hydrolysis by PLA_2 are still a subject of debate. A number of investigators have suggested that the global structures of various phospholipid vesicular substrates do not change, even after hydrolysis of the outer monolayer (Jain et al., 1980; Jones and Hunt, 1985; Wilschut et al., 1979). Biltonen et al., on the other hand, claim that vesicles undergo a large shape change and even burst after a critical mole fraction of reaction products has accumulated within the bilayer (Burack and Biltonen, 1994). In the case of $DC_{8,9}PC$ tubules, the presence of fractured and unwrapped tubules after partial PLA_2 hydrolysis suggests that the preferred crystal structure of the hydrolysis products is incompatible with that of the substrate $DC_{8,9}PC$. Tubules appear to remain intact until a certain fraction of reaction products is reached within a local region of the tubule bilayer. As observed from fluorescence microscopy, at the point when product accumulation can no longer support the specific asymmetrical curvature required to form a 1-μm-diameter tubule, the product regions fracture and unwrap to form smaller helices, filaments, and flat sheets.

It has long been recognized that phospholipases are highly sensitive to the "quality" of the interface (Burack and Biltonen, 1994; Gelb et al., 1995; Jain et al., 1995), and, especially for this model system, the kinetics depend intimately on the spatial and temporal distribution of packing domains within the tubule. The linear kinetics must arise as a consequence of the cylindrical geometry of a tightly packed, crystalline array of phospholipids because SUVs do not give rise to linear kinetics. The exact molecular mechanism remains elusive. The distribution of defects along the tubular microstructure, the influence of a high axial ratio geometry on the diffusion trajectories of enzyme, and the recruitment of new enzyme into spatially isolated, product-rich domains during hydrolysis are possible mechanisms currently under investigation in our laboratory.

We propose that PLA_2 initially binds (with low affinity) everywhere on the solvent-exposed regions of the tubule, but hydrolysis begins only in regions in which the tight crystal lattice is disturbed and where lipids adopt conformations that are more susceptible to enzymatic attack. Hydrolysis then proceeds outward from defects along the surface, and localized domains of product begin to form. PLA_2 binds with greater affinity to anionic bilayers than to zwitterionic bilayers (Jain et al., 1982, 1986), and, as such, PLA_2 binds more tightly to these negatively charged regions of tubule, which contain product. Hydrolysis continues at the boundaries between product domains and domains of fresh substrate. Because of the geometrical constraints of a cylindrical structure, the hydrolysis boundary between fresh and depleted substrate eventually reaches a limiting size. Further recruitment of enzyme to a region rich in product does little to affect the rate of hydrolysis, because access to fresh substrate becomes increasingly limited. At this point, the rate remains constant as a growing hydrolysis front proceeds down the length of the tubule. The differential binding affinity of PLA_2 to uncharged substrate and anionic product domains within bilayers of zwitterionic phosphatidylcholine vesicles has been cited as one possible origin of the "lag phase" observed in the hydrolysis of these lipids (Berg et al., 1991). Later in the reaction, the molecular packing of hydrolysis products can no longer sustain the high free energy of bending needed to maintain the curvature of the mostly hydrolyzed tubule. The bilayer fractures along line defects and unravels into sheets and helical ribbons, which ultimately tear to become smaller helical ribbons and filaments.

The zero-order degradation profile for this model system suggests that self-assembled tubule microstructures may function as controlled release drug delivery systems, and current work aims at developing this and other self-assembled tubule systems into a new drug delivery technology. Although the large dimensions of lipid tubules suggest that they will be of restricted utility in delivery of drugs from within the vasculature, they are ideally suited for use at intramuscular, subcutaneous, intraperitoneal, topical, and intratumor sites in which localization of the drug delivery system is desirable. These results demonstrate that even with a tightly packed crystalline microstructure, lipid tubules can be degraded by enzymatic hydrolysis, albeit at a slow rate. Future tubule designs will include water-soluble drugs covalently attached to the headgroups of tubule-forming lipids, which should lead to release from the microstructures upon hydrolysis. This form of chemical delivery has great potential and may intrinsically allow for the protection of labile peptide drugs from premature hydrolysis due to the tight molecular packing of the crystalline bilayer. Only lipids at phase boundaries and crystal edges, like those at tubule ends, may be accessible to enzymatic attack. From steric considerations, small, hydrophilic peptides and prodrugs seem to have the most promise, but mixed lipid tubule formations may accommodate prodrug lipids with headgroups as large as small proteins. How the packing of lipids with drug-bearing headgroups affects tubule formation, the rate of enzymatic hydrolysis, and drug release by dissolution is currently under investigation.

We acknowledge the support of the National Institutes of Health Research Training in Biotechnology grant (GM-08437), the University of Washington Royalty Research Fund, and the Whitaker Foundation for this research.

REFERENCES

Berg, O. G., B. Z. Yu, J. Rogers, and M. K. Jain. 1991. Interfacial catalysis by phospholipase A_2: determination of the interfacial rate constants. *Biochemistry.* 30:7283–97.

Burack, W. R., and R. L. Biltonen. 1994. Lipid bilayer heterogeneities and modulation of phospholipase A_2 activity. *Chem. Phys. Lipids.* 73: 209–222.

Burack, W. R., Q. Yuan, and R. L. Biltonen. 1993. Role of lateral phase separation in the modulation of phospholipase A_2 activity. *Biochemistry.* 32:583–589.

Caffrey, M., J. Hogan, and A. S. Rudolph. 1991. Diacetylenic lipid microstructures: structural characterization by x-ray diffraction and comparison with the saturated phosphatidylcholine analogue. *Biochemistry.* 30:2134–2146.

Chappell, J. S., and P. Yager. 1991. A model for crystalline order within helical and tubular structures of chiral bilayers. *Chem. Phys. Lipids.* 58:253–258.

Gelb, M. H., M. K. Jain, A. M. Hanel, and O. G. Berg. 1995. Interfacial enzymology of glycerolipid hydrolases: lessons from secreted phospholipases A_2. *Annu. Rev. Biochem.* 64:653–688.

Georger, J., R. Price, A. Singh, J. M. Schnur, P. E. Schoen, and P. Yager. 1987. Helical and tubular microstructures formed by polymerizable phosphatidylcholines. *J. Am. Chem. Soc.* 109:6169–6175.

Grainger, D. W., A. Reichert, H. Ringsdorf, and C. Salesse. 1990. Hydrolytic action of phospholipase A_2 in monolayers in the phase transition region: direct observation of enzyme domain formation using fluorescence microscopy. *Biochim. Biophys. Acta.* 1023:365–379.

Jain, M. K., M. R. Egmond, H. M. Verheij, R. Apitz-Castro, R. Dijkman, and G. H. DeHaas. 1982. Interaction of phospholipase A_2 and phospholipid bilayers. *Biochim. Biophys. Acta.* 688:341–8.

Jain, M. K., M. H. Gelb, J. Rodgers, and O. G. Berg. 1995. Kinetic basis for interfacial catalysis by phospholipase A_2. *Methods Enzymol.* 249: 567–614.

Jain, M. K., B. P. Maliwal, G. H. DeHaas, and A. J. Slotboom. 1986. Anchoring of phospholipase A_2: the effect of anions and deuterated water, and the role of N-terminus region. *Biochim. Biophys. Acta.* 860:448–61.

Jain, M. K., C. J. A. van Echfeld, F. Ramirez, J. de Gier, G. H. de Haas, and L. L. M. van Deenen. 1980. Association of lysophosphatidylcholine with fatty acids in aqueous phase to form bilayers. *Nature.* 284: 486–487.

Jones, I. C., and G. R. Hunt. 1985. A ^{31}P- and ^{1}H-NMR investigation into the mechanism of bilayer permeability induced by the action of phospholipase A_2 on phosphatidylcholine vesicles. *Biochim. Biophys. Acta.* 820:48–57.

Mabrey, S., and J. M. Sturtevant. 1977. Incorporation of saturated fatty acids into phosphatidylcholine bilayers. *Biochim. Biophys. Acta.* 486: 444–450.

Maloney, K. M., M. Granbois, D. W. Grainger, C. Salesse, K. A. Lewis, and M. F. Roberts. 1995. Phospholipase A_2 domain formation in hydrolyzed asymmetric phospholipid monolayers at the air/water interface. *Biochem. Biophys. Acta.* 1235:395–405.

Plant, A. L., D. M. Benson, and G. L. Trusty. 1990. Probing the structure of diacetylenic phospholipid tubules with fluorescent lipophiles. *Biophys. J.* 57:925–933.

Reichert, A., H. Ringsdorf, and A. Wagenknecht. 1992. Spontaneous domain formation of phospholipase A_2 at interfaces: fluorescence microscopy of the interaction of phospholipase A_2 with mixed monolayers of lecithin, lysolecithin and fatty acid. *Biochim. Biophys. Acta.* 1106: 178–188.

Richieri, G. V., A. Anel, and A. M. Kleinfeld. 1993. Interactions of long-chain fatty acids and albumin: determination of free fatty acid levels using the fluorescent probe ADIFAB. *Biochemistry.* 32: 7574–7580.

Richieri, G. V., R. T. Ogata, and A. M. Kleinfeld. 1992. A fluorescently labeled intestinal fatty acid binding protein. Interactions with fatty acids and its use in monitoring free fatty acids. *J. Biol. Chem.* 267: 23495–23501.

Schnur, J. M. 1993. Lipid tubules: a paradigm for molecularly engineered structures. *Science.* 262:1669–1676.

Schnur, J. M., R. R. Price, P. Schoen, P. Yager, J. M. Calvert, J. Georger, and A. Singh. 1987. Lipid-based tubule microstructures. *Thin Solid Films.* 152:181–206.

Selinger, J. V., and J. M. Schnur. 1993. Theory of chiral lipid tubules. *Phys. Rev. Lett.* 71:4091–4094.

Small, D. M. 1986. The physical chemistry of lipids. *In* Handbook of Lipid Research, Vol. 4. Plenum Press, New York. 672 pp.

Thomas, B. N., C. R. Safinya, R. J. Plano, and N. A. Clark. 1995. Lipid tubule self-assembly: length dependence on cooling rate through a first-order phase transition. *Science.* 267:1635–1638.

Wilschut, J. C., J. Regts, and G. Scherphof. 1979. Action of phospholipase A_2 on phospholipid vesicles. Preservation of the membrane permeability barrier during asymmetric bilayer degradation. *FEBS Lett.* 98:181–186.

Wilschut, J. C., J. Regts, H. Westenberg, and G. Scherphof. 1978. Action of phospholipases A_2 on phosphatidylcholine bilayers: effects of the phase transition, bilayer curvature and structural defects. *Biochim. Biophys. Acta.* 508:185–196.

Yager, P., and P. Schoen. 1984. The formation of tubules by a polymerizable surfactant. *Mol. Cryst. Liq. Cryst.* 106:371–381.